

# Maximal-Ratio Eigen-Combining for Smarter Antenna Arrays

Constantin Siriteanu and Steven D. Blostein, *Senior Member, IEEE*

**Abstract**—In typical mobile wireless scenarios, signals are received with power azimuth angle spectrum (p.a.s.) of variable azimuth angle spread (AS). Therefore, conventional maximum average signal-to-noise ratio beamforming (BF) or maximal-ratio combining (MRC) may not necessarily be effective in terms of performance or signal processing complexity. A newer, more flexible, approach, called maximal-ratio eigen-combining (MREC) is analyzed and found to generalize BF and MRC. For imperfectly-known channels we study both suboptimal and optimal eigen-/combining. MREC-based analysis is shown to simplify MRC performance investigations for correlated channel gains. For MPSK signals, we present average error probability (AEP) expressions for MREC, BF, and MRC, that are new or generalizations of our previous work. Furthermore, we propose a performance–complexity tradeoff criterion (PCTC) for MREC-receiver adaptation to changing AS. Numerical evaluations for typical urban scenarios with realistic Laplacian p.a.s. of random AS demonstrate that PCTC-based MREC is an interesting alternative to BF and MRC, for smart antenna arrays.

**Index Terms**—Array signal processing, diversity methods, eigen-combining, fading channels.

## I. INTRODUCTION

IN mobile wireless communications, received signals are characterized by power azimuth angle spectrum (p.a.s.) [1], [2] with variable azimuth spread (AS) [3]. This changes the correlation between signals received at the antenna array elements [1], [4]. As a result, for traditional combining methods such as maximum average signal-to-noise ratio (SNR) beamforming (BF) [5] and maximal-ratio combining (MRC) [6], [7], symbol detection performance varies, while algorithm complexity (and thus receiver power consumption) remains constant.

A more flexible approach is maximal-ratio eigen-combining (MREC) [8]–[15] which consists of the Karhunen-Loève Transform (KLT) [12] followed by MRC. Numerical results from lengthy simulations [11], [13], or from analysis for unrealistic channel characteristics (e.g., uniform p.a.s.) [8], [9], suggest that MREC adapted to channel scattering geometry can outperform BF and even MRC, and can lower complexity

Manuscript received December 14, 2004; revised October 30, 2005; accepted May 10, 2006. The associate editor coordinating the review of this paper and approving it for publication was X. Wang. This research is supported by grants from Samsung AIT, Korea, as well as from Bell Mobility, Canada.

C. Siriteanu was with the Department of Electrical and Computer Engineering, Queen's University, Kingston, Canada. He is now with the HY-SDR Research Centre, Hanyang University, Seoul, South Korea (e-mail: costi@dsplab.hanyang.ac.kr).

S. D. Blostein is Head of the Department of Electrical and Computer Engineering, Queen's University, Kingston, Canada (e-mail: steven.blostein@queensu.ca).

Digital Object Identifier 10.1109/TWC.2007.04883.

compared to MRC. Nevertheless, previously-proposed MREC adaptation criteria [12], [14] disregard the channel estimation method and its parameters, and, even worse, MREC performance and complexity.

Using channel estimates as in the traditional combining approach [7], [16], [17], which we refer to as *approximate MRC* [8]–[10], because it yields suboptimal performance, has complicated analysis even for BPSK signals when branches are not independent identically distributed (i.i.d.) [7], [8], [10], [16]–[22]. On the other hand, analysis of optimum combining for estimated channels [20], [23], i.e., *exact MRC* [9], is straightforward for i.i.d. branches and MPSK signals [23]. Both approaches were applied to eigen-combining in [8], [9], for BPSK.

In this paper we provide a comprehensive performance/complexity analysis of exact and approximate MREC, BF, and MRC, when the channel is estimated based on pilot-symbol-aided modulation (PSAM) [24] and interpolation [8]–[10]. We make the following contributions:

- performance/complexity studies for suboptimal and optimal eigen-/combining are presented, and previous results [9] are generalized.
- equivalences between MREC, BF, and MRC are proved, and exploited to simplify BF and MRC analysis for correlated, imperfectly-known, channel gains.
- a novel approximate-MRC average error probability (AEP) expression for MPSK and i.i.d. branches, that is much simpler than a previous result [7, Appendix C, Eqn. C-16], is derived based on exact-MRC.
- the effectiveness of a novel performance–complexity tradeoff criterion (PCTC) for MREC adaptation is demonstrated for typical urban (TU) scenarios with Laplacian p.a.s. and random AS variation.

This paper is organized as follows: Section II contains the received signal model; suboptimal and optimal combining and eigen-combining are analyzed in Section III; MREC adaptation criteria are discussed in Section IV, and numerical results are presented in Section V.

## II. SIGNAL MODEL

Consider a mobile station transmitting an MPSK signal through a frequency-flat Rayleigh fading channel and an  $L$ -element receiving base-station antenna array. After demodulation, matched-filtering and symbol-rate sampling, the complex-valued received signal vector is

$$\tilde{\mathbf{y}} = \sqrt{E_s} \mathbf{b} \tilde{\mathbf{h}} + \tilde{\mathbf{n}}, \quad (1)$$

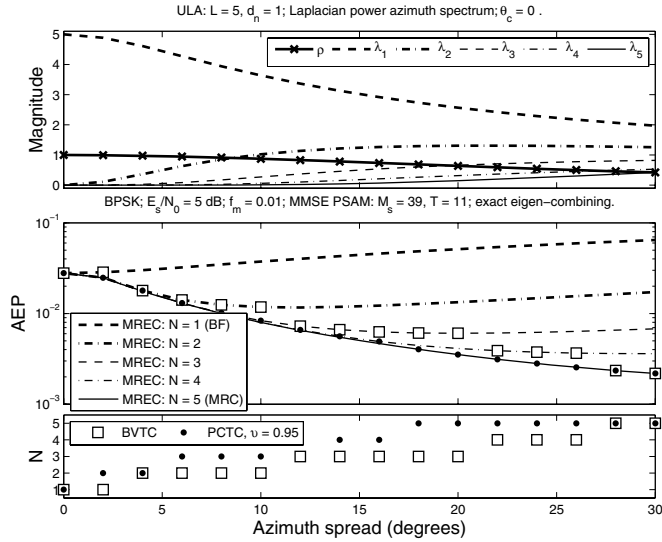


Fig. 1. Top: fading correlation for adjacent antenna elements,  $\rho$ , and channel correlation matrix eigenvalues,  $\lambda_i$ ,  $i = 1 : L$ ; Middle: exact-MREC AEPs for BPSK and MMSE PSAM eigengain estimation; BF performs poorly for non-zero AS; MRC-like performance can be achieved with MREC, at much lower complexity; Bottom: MREC order selected with criteria described in Section IV.

whose dependence on the sampling time is not explicit, to simplify notation. The  $L$  elements  $\tilde{y}_i$ ,  $i = 1 : L \triangleq 1, \dots, L$ , of the received signal vector  $\tilde{\mathbf{y}} = [\tilde{y}_1 \tilde{y}_2 \dots \tilde{y}_L]^T$ , are called *branches*, and the elements  $h_i$ ,  $i = 1 : L$ , of the channel vector  $\tilde{\mathbf{h}} = [h_1 h_2 \dots h_L]^T$ , are called *channel gains*. In (1),  $E_s$  is the energy transmitted per symbol, and  $b$  is the transmitted MPSK symbol, with  $|b|^2 = 1$ . We assume that the channel vector  $\tilde{\mathbf{h}}$  and the noise vector  $\tilde{\mathbf{n}}$  are complex-valued, mutually independent, zero-mean Gaussian, with  $\tilde{\mathbf{h}} \sim \mathcal{CN}(\mathbf{0}, \mathbf{R}_{\tilde{\mathbf{h}}})$  and  $\tilde{\mathbf{n}} \sim \mathcal{CN}(\mathbf{0}, N_0 \mathbf{I}_L)$ . Further assumptions are that the channel fading is frequency-flat, the noise is temporally-white, and the received signal is interference-free. The numerical results shown in this work are for channel gains with unit variance.

In cellular wireless communications systems, wave scattering induces azimuthal angle dispersion [1]–[3]. The channel's spatial selectivity, i.e., the antenna decorrelation [1], [4], is affected by the power azimuth spectrum (p.a.s.), defined in [3, Eqn. 2], and its root second central moment, denoted as azimuth spread (AS) [3], [4]. The numerical results presented herein assume a truncated Laplacian p.a.s. [4, Eqn. 12], which accurately models measurements for most actual scenarios [3], unlike the uniform and Gaussian p.a.s. [1], [4]. Straightforward mathematical operations can produce closed-form expressions for the elements of  $\mathbf{R}_{\tilde{\mathbf{h}}}$  [4], [10].

For a uniform linear array (ULA) with  $L = 5$ , normalized inter-element distance  $d_n = 1$  (i.e., the physical distance equals half the carrier wavelength), and for average angle of arrival (AoA)  $\theta_c = 0^\circ$  (with respect to antenna broadside), the top subplot in Fig. 1 shows the correlation,  $\rho$ , between any two adjacent antennas, and the eigenvalues of  $\mathbf{R}_{\tilde{\mathbf{h}}}$ ,  $\lambda_i$ ,  $i = 1 : L$ , vs. the AS. Clearly, the AS determines antenna correlation and the relative eigenvalue magnitudes. For small AS, the received signals are highly correlated, and the received signal energy, proportional to  $\text{tr}(\mathbf{R}_{\tilde{\mathbf{h}}}) \triangleq \sum_{i=1}^L (\mathbf{R}_{\tilde{\mathbf{h}}})_{i,i} = \sum_{i=1}^L \lambda_i$ ,

TABLE I  
MOBILE, CHANNEL, AND RECEIVER (CHANNEL ESTIMATION)  
PARAMETERS.

Parameter	Value
Mobile speed	$v = 60$ km/h
Transmitted BPSK symbol rate	$f_s = 10$ ksp/s
Carrier frequency	$f_c = 1.8$ GHz
Pilot symbol period [24, Sect. III.C]	$M_s = 39$
Maximum Doppler frequency	$f_D = 100$ Hz
Normalized max. Doppler frequency	$f_m = f_D/f_s = 0.01$
Channel coherence time [25, Eqn. 4.40.b]	$T_c \approx 1.8$ ms
Channel coherence distance	$d_c = vT_c \approx 30$ mm
Interpolator size [24, Sect. III.D]	$T = 11$

is concentrated along the first few eigen-directions. Then, the channel is said to be spatially non-selective and the available diversity gain is small [12]. When the AS increases, antenna correlation decreases, the channel becomes spatially more selective, and higher diversity gain becomes available. In subsequent sections we show how to exploit available diversity gain within computational constraints.

The AS depends on the environment and antenna array location and height, and is time-varying [3]. Measurements for sub/urban scenarios [3] showed that the base-station AS can be well-modeled as a random variable with log-normal distribution, i.e.,

$$AS = 10^{\epsilon x + \mu}; \quad x \sim \mathcal{N}(0, 1). \quad (2)$$

For numerical results shown hereafter we set  $\mu = 0.74$  and  $\epsilon = 0.47$ , as empirically determined in [3] for a typical urban (TU) scenario, with uniform density of 4–6-storey buildings, irregular street layout, 0.2–1.1 km distance between the mobile station and the base station, no line of sight, and receiving antenna array positioned above rooftop level. Then, AS is predominantly small-to-moderate, i.e.,  $Pr(1^\circ < AS < 20^\circ) \approx 0.8$  [2], [3], with spatial correlation given by [3]

$$\rho_{AS}(d) = e^{-d/d_{AS}}, \quad (3)$$

where  $d$  is the distance traveled by the mobile station, and  $d_{AS}$  is the AS *decorrelation distance*, i.e., the distance for which AS correlation decreases by a factor of two [3]. Measurements found  $d_{AS} = 50$  m for this TU scenario [3]. By comparison, the fading coherence distance [25, Eqn. 4.40.b],  $d_c$ , given for typical system parameter values in Table I, is 3 orders of magnitude shorter.

### III. MAXIMAL-RATIO EIGEN-COMBINING (MREC)

#### A. Optimum Eigen-/Combining for Perfectly-Known Channels

1) *Maximal-Ratio Eigen-Combining for Perfectly-Known Channel — Ideal MREC*: The channel correlation matrix  $\mathbf{R}_{\tilde{\mathbf{h}}}$  has real non-negative eigenvalues  $\lambda_1 \geq \lambda_2 \geq \dots \geq \lambda_L \geq 0$ , orthonormal eigenvectors,  $\mathbf{e}_i$ ,  $i = 1 : L$ , and can be decomposed as  $\mathbf{R}_{\tilde{\mathbf{h}}} = \mathbf{E}_L \mathbf{\Lambda}_L \mathbf{E}_L^H$ , where  $\mathbf{\Lambda}_L \triangleq \text{diag}\{\lambda_i\}_{i=1}^L$  is a diagonal matrix, and  $\mathbf{E}_L \triangleq [\mathbf{e}_1 \mathbf{e}_2 \dots \mathbf{e}_L]$  is a unitary matrix. Hereafter,  $\mathbf{R}_{\tilde{\mathbf{h}}}$ ,  $\mathbf{\Lambda}_L$ , and  $\mathbf{E}_L$  are assumed perfectly-known because, in practice, enough independent channel samples

would be available for accurate estimation [11], since AS varies slowly compared to the fading.

Ideal maximal-ratio eigen-combining (MREC) of order  $N$ ,  $1 \leq N \leq L$ , consists of two steps:

- (i) The  $L \times N$ , full column rank matrix  $\mathbf{E}_N \triangleq [\mathbf{e}_1 \mathbf{e}_2 \dots \mathbf{e}_N]$  transforms (1) into

$$\mathbf{y} = \sqrt{E_s} b \mathbf{h} + \mathbf{n}, \quad (4)$$

where  $\mathbf{y} \triangleq \mathbf{E}_N^H \tilde{\mathbf{y}}$ ,  $\mathbf{h} \triangleq \mathbf{E}_N^H \tilde{\mathbf{h}}$ ,  $\mathbf{n} \triangleq \mathbf{E}_N^H \tilde{\mathbf{n}}$ .

- (ii) The eigenbranches, i.e., the elements of  $\mathbf{y}$ , are linearly combined so as to maximize the instantaneous output SNR (i.e., the maximal-ratio criterion [6]) using

$$\mathbf{w}_{\text{MREC}} = \mathbf{h}. \quad (5)$$

The elements of  $\mathbf{h}$  are denoted further as *eigengains*. They are mutually uncorrelated, with zero mean, and variances

$$\sigma_{h_i}^2 \triangleq E\{|h_i|^2\} = \lambda_i, \quad (6)$$

i.e.,  $\mathbf{R}_h \triangleq E\{\mathbf{h}\mathbf{h}^H\} = \mathbf{\Lambda}_N = \text{diag}\{\lambda_i\}_{i=1}^N$ , for any channel gain distribution [12]. From the initial assumptions on fading and noise, we obtain  $\mathbf{n} \sim \mathcal{CN}(\mathbf{0}, N_0 \mathbf{I}_N)$ , and  $\mathbf{h} \sim \mathcal{CN}(\mathbf{0}, \mathbf{\Lambda}_N)$ , so that the eigengains are independent.

The transformation leading to (4) is the Karhunen-Loève Transform (KLT) [12]. Of all possible transforms, the KLT packs the largest amount of energy from the original,  $L$ -dimensional, signal vector  $\tilde{\mathbf{y}}$ , into the transformed,  $N$ -dimensional, signal vector  $\mathbf{y}$ , which is desirable for dimension reduction [14].

Using eigenbranch independence, the approach in [19, Chapter 9] applied for the moment generating function (m.g.f.) of the MREC-output SNR yields the following AEP expression for order- $N$  ideal MREC, MPSK, and branches that can be non-i.i.d. [8, Eqn. 11]

$$P_{e,N} = \frac{1}{\pi} \int_0^{\frac{M-1}{M}\pi} \prod_{i=1}^N \left( 1 + \frac{E_s}{N_0} \lambda_i \frac{g_{\text{PSK}}}{\sin^2 \phi} \right)^{-1} d\phi, \quad (7)$$

where

$$g_{\text{PSK}} \triangleq \sin^2 \frac{\pi}{M}. \quad (8)$$

2) *Relation to Ideal BF and MRC*: For  $N = 1$ , MREC reduces to BF [12], [14], where the inner product of the original received signal vector with a vector proportional to the eigenvector of  $\mathbf{R}_h$  corresponding to its largest eigenvalue is taken [5]. It is known that BF can provide maximum  $10 \log_{10} L$  dB antenna gain [5], [12], for coherent branches. However, BF cannot exploit diversity gain in spatially-selective channels [12], [13], unlike higher-order MREC [8]–[10]. The BF AEP is given by (7) for  $N = 1$ , which can also be recast in closed-form [8, p. 17], [10].

For perfectly-known channel gains, MRC [6] is equivalent to MREC of order  $N = L$  [26], [27], denoted as *full MREC*. Thus, for  $N = L$ , Eqn. (7) is the AEP expression for ideal MRC, for branches that can be correlated and non-identically distributed. (An analogous equivalence does not hold for diversity combining techniques such as equal-gain or selection combining [27].)

## B. Channel Estimation using Pilot-Symbol-Aided Modulation (PSAM)

A practical method to estimate the eigen/gains is as follows [24]: the transmitter inserts one known pilot symbol every  $M_s$  symbols, an approach known as pilot-symbol-aided modulation (PSAM); then, the receiver estimates the channel fading corresponding to data symbols by interpolating between  $T$  pilot samples acquired across slots. Refer to [8]–[10] for details on two such estimation methods denoted as SINC PSAM (data-independent, simple, suboptimal, with poor performance in low SNR) and MMSE PSAM (minimum mean-squared-error interpolation; data-dependent, complex, optimal).

## C. Suboptimal Eigen-/Combining for Imperfectly-Known Channels

In Section III-A above, we assumed perfect knowledge of  $\mathbf{R}_h$  (thus of  $\mathbf{E}_L, \mathbf{\Lambda}_L$ ), and the eigen/gains. Hereafter, we relax the assumption regarding the latter, and denote the estimators of  $\tilde{h}_i$  and  $h_i$  as  $\tilde{g}_i$  and  $g_i$ , respectively,  $i = 1 : L$ .

1) *Suboptimal Combining given Estimates of the Channel Gains — Approximate MRC*: For the signal model (1), when individual channel gains are estimated, a standard approach (see [7, Appendix C], [15]–[17] [19, Section 9.9], [20]–[22] and references therein) is to detect symbols using the test variable

$$\tilde{q} \triangleq \tilde{\mathbf{g}}^H \tilde{\mathbf{y}}, \quad \text{where} \quad (9)$$

$$\tilde{\mathbf{g}} \triangleq [\tilde{g}_1 \ \tilde{g}_2 \ \dots \ \tilde{g}_L]^T, \quad (10)$$

i.e., the receiver uses the channel gain estimates as if they coincide with the actual gains. This approach is denoted *approximate MRC* [9], [10] due to its suboptimality [20, Section III].

2) *Previous Approximate-MRC Analyses, for MPSK, and I.I.D. Branches*: Traditionally, analyses of approximate MRC for BPSK modulation and i.i.d. branches have relied on:

- the *characteristic function of the test variable*  $\tilde{q}$  we defined in (9) [7, Appendix C], [16]. The lengthy, yet straightforward, derivation in [16] lead to a simple closed-form AEP expression [16, Eqn. 59]. Involved derivations lead to an equivalent closed-form AEP expression [7, Appendix C, Eqn. C-18].
- the *pdf of the combiner-output SNR* [17]. Such an approach [18] was recently shown to only yield an error probability lower bound [21, Section II]. In [21], the AEP expression from [16, Eqn. 59] was re-derived, still using the test variable  $\tilde{q}$ , and the convenient fading estimate model from [17, Eqn. 16].

For other PSK constellations, a previous performance study of approximate MRC of i.i.d. branches is involved and produced a complicated, non-closed-form symbol-AEP expression [7, Appendix C, Eqn. C-16]. We present a simpler approach and AEP expression in Section III-E.1.

3) *Previous Approximate-MRC Analyses, for BPSK, and Non-I.I.D. Branches*: The approach in [16] was rediscovered and applied for non-i.i.d. branches in [20], although explicit AEP expressions were not provided. A finite-limit integral AEP expression [22, Eqn. 19], found by reinterpreting results

from [7, Appendix B] [19, Appendix 9A], is claimed to apply to BPSK modulation, even for non-i.i.d. fading. However, the assumption in [22, Eqn. 2] regarding the relation between a channel gain and its estimate can limit the applicability of these results to the case of i.i.d. branches. Our Section III-C.5 and Appendix describe a more comprehensive performance analysis approach and AEP expression.

4) *Suboptimal Eigen-Combining given Estimates of the Eigengains — Approximate MREC*: This approach [8], [10], [12], [14], [15] uses for symbol detection the test statistic

$$q \triangleq \mathbf{g}^H \mathbf{y}, \quad \text{where} \quad (11)$$

$$\mathbf{g} \triangleq [g_1 \ g_2 \ \cdots \ g_N]^T. \quad (12)$$

Statistical independence of the eigenbranches allows for a straightforward analysis of approximate MREC [8] based on the approach in [16], [20], although casting the AEP in closed-form is tedious [8]. For completeness, an abridged version of our derivation from [8] appears in the Appendix. The involved, closed-form, approximate-MREC AEP expression derived in [8] appears as Eqn. (37) in the Appendix. It can be used to confirm that for highly-correlated branches approximate-MREC performance can degrade with increasing order [8], [12], [14], [15].

5) *Relation to BF and MRC for Approximate Eigen-/Combining*: Since for  $N = 1$  approximate MREC reduces to BF [5], [13], an approximate-BF AEP expression is (37), with  $N = 1$ .

If the same linear estimation method, e.g., SINC/MMSE PSAM [8], is used before and after the KLT then, for  $N = L$ ,

$$\mathbf{g} = \mathbf{E}_L^H \tilde{\mathbf{g}}. \quad (13)$$

As  $\mathbf{y} = \mathbf{E}_L^H \tilde{\mathbf{y}}$ , the test statistics for approximate full MREC and MRC coincide, i.e.,

$$q = \mathbf{g}^H \mathbf{y} = \tilde{\mathbf{g}}^H \tilde{\mathbf{y}} = \tilde{q}, \quad (14)$$

proving their performance-equivalence, which we confirmed by simulation in [8], [10]. Hence, Eqn. (37) with  $N = L$ , is also the AEP expression for BPSK and approximate MRC of non-i.i.d. branches, and the most comprehensive such result known to the authors.

#### D. Optimal Eigen-/Combining for Imperfectly-Known Channels

Optimal eigen-/combining given estimated eigen/gains, which we term *exact MREC/MRC* [9], [10], has rarely been considered before [9], [20], [23], although it can provide useful performance limits. Exact-MRC implementation and analysis are tedious for correlated gains [10], [20], even for BPSK. The opposite is true for uncorrelated gains even for MPSK [23]. In the following, we expand on the exact-MREC work we initiated in [9].

1) *Optimal Eigen-Combining given Estimates of the Eigengains — Exact MREC*: For zero-mean, jointly-Gaussian  $\mathbf{h}$  and  $\mathbf{g}$  (a common assumption also found in [7], [17], [21], [23] for estimates obtained from pilot samples), the distribution of

the channel gain vector conditioned on its estimate is given by  $\mathcal{CN}(\mathbf{m}, \mathbf{R}_e)$ , where [28, Appendix 15B, p. 562]

$$\mathbf{m} \triangleq E\{\mathbf{h}|\mathbf{g}\} = E\{\mathbf{h}\mathbf{g}^H\} [E\{\mathbf{g}\mathbf{g}^H\}]^{-1} \mathbf{g}, \quad (15)$$

$$\begin{aligned} \mathbf{R}_e &\triangleq E\{(\mathbf{h} - \mathbf{m})(\mathbf{h} - \mathbf{m})^H|\mathbf{g}\} \\ &= \mathbf{R}_h - E\{\mathbf{h}\mathbf{g}^H\} [E\{\mathbf{g}\mathbf{g}^H\}]^{-1} E\{\mathbf{g}\mathbf{h}^H\}, \end{aligned} \quad (16)$$

so that

$$\mathbf{h} = \mathbf{m} + \mathbf{e}, \quad (17)$$

with  $\mathbf{e} \sim \mathcal{CN}(\mathbf{0}, \mathbf{R}_e)$ . Thus, from (4), we have

$$\mathbf{y} = \sqrt{E_s} b \mathbf{m} + \boldsymbol{\nu} \sim \mathcal{CN}(\sqrt{E_s} b \mathbf{m}, \mathbf{R}_\nu) \quad (18)$$

where  $\boldsymbol{\nu} \triangleq \sqrt{E_s} b \mathbf{e} + \mathbf{n}$ , and  $\mathbf{R}_\nu \triangleq E\{\boldsymbol{\nu}\boldsymbol{\nu}^H\} = E_s \cdot \mathbf{R}_e + N_0 \cdot \mathbf{I}_N$ , for MPSK transmitted symbols.

Eigenbranch independence causes the elements of  $\mathbf{g}$  to be independent, and the above correlation matrices to be diagonal. Based on (15), (16), and (6),  $m_i = \frac{\sigma_{h_i, g_i}^2}{\sigma_{g_i}^2} g_i$  and  $(\mathbf{R}_\nu)_{i,i} = E_s \left( \lambda_i - \frac{|\sigma_{h_i, g_i}^2|^2}{\sigma_{g_i}^2} \right) + N_0$ , where  $\sigma_{h_i, g_i}^2 \triangleq E\{h_i g_i^*\}$  (assumed real-valued, positive — see [7, p. 954], [16, p. 34]) and  $\sigma_{g_i}^2 \triangleq E\{|g_i|^2\}$ . The expressions for these correlations are shown in [8, Tables 2,3] for SINC/MMSE PSAM. The SNR for the  $i$ th element of the conditioned signal vector in (18) is

$$\gamma_i \triangleq E_s \frac{|m_i|^2}{(\mathbf{R}_\nu)_{i,i}} = \frac{\frac{E_s}{N_0} \lambda_i |\mu_i|^2}{\frac{E_s}{N_0} \lambda_i (1 - |\mu_i|^2) + 1} \cdot \frac{|g_i|^2}{\sigma_{g_i}^2}. \quad (19)$$

where  $\mu_i$  is the correlation coefficient of  $h_i$  and  $g_i$  defined as

$$\mu_i \triangleq \frac{E\{h_i g_i^*\}}{\sqrt{E\{|h_i|^2\} E\{|g_i|^2\}}} = \frac{\sigma_{h_i, g_i}^2}{\sqrt{\sigma_{h_i}^2 \sigma_{g_i}^2}}. \quad (20)$$

The maximum-likelihood combiner for the signal model in (18) is

$$\mathbf{w}_{e,N} = \mathbf{R}_\nu^{-1} \mathbf{m}. \quad (21)$$

The output SNR conditioned on the eigengain estimates, i.e., the SNR in  $\mathbf{w}_{e,N}^H \mathbf{y}$ , is then

$$\gamma = E_s \mathbf{m}^H \mathbf{R}_\nu^{-1} \mathbf{m} = E_s \sum_{i=1}^N \frac{|m_i|^2}{(\mathbf{R}_\nu)_{i,i}} = \sum_{i=1}^N \gamma_i, \quad (22)$$

i.e., maximum [6], motivating the term “exact MREC” for this approach. From (21), (15) and (16), the individual weights for exact MREC are

$$[\mathbf{w}_{e,N}]_i = \frac{1}{\frac{E_s}{N_0} \lambda_i (1 - |\mu_i|^2) + 1} \frac{\sigma_{h_i, g_i}^2}{\sigma_{g_i}^2} g_i, \quad i = 1 : N. \quad (23)$$

Besides  $g_i$ , which is a weight for approximate MREC, the weights in (23) require an additional factor which depends on fading and noise statistics.

As shown in the Appendix, for BPSK, approximate MREC yields to a straightforward test-variable-based analysis which, however, produces the complicated AEP expression from (37). On the other hand, for exact MREC, the independence of  $\gamma_i$ ,  $i = 1 : N$ , coupled with (22), allows for the following conditioned-SNR-based AEP analysis [23] that produces a simple, insightful, and helpful AEP expression.

For MPSK transmitted signals and order- $N$  exact MREC, the symbol error probability conditioned on  $\gamma$  can be written as [19, Eqn. 8.22]

$$P_{e,N}(\gamma) = \frac{1}{\pi} \int_0^{\frac{M-1}{M}\pi} \exp\left\{-\gamma \frac{g_{\text{PSK}}}{\sin^2 \phi}\right\} d\phi. \quad (24)$$

Then, the symbol-AEP is [19]

$$P_{e,N} \triangleq E\{P_{e,N}(\gamma)\} = \frac{1}{\pi} \int_0^{\frac{M-1}{M}\pi} M_\gamma\left(-\frac{g_{\text{PSK}}}{\sin^2 \phi}\right) d\phi. \quad (25)$$

where  $M_\gamma(s) \triangleq E\{e^{s\gamma}\}$  is the m.g.f. of  $\gamma$ . Using (22) and the independence of  $\gamma_i$ ,  $i = 1 : L$ , Eqn. (25) becomes

$$P_{e,N} = \frac{1}{\pi} \int_0^{\frac{M-1}{M}\pi} \prod_{i=1}^N M_{\gamma_i}\left(-\frac{g_{\text{PSK}}}{\sin^2 \phi}\right) d\phi. \quad (26)$$

Since  $g_i$  is Gaussian, the conditioned SNR  $\gamma_i$  from (19) is exponentially distributed [19, Eqn. 2.7], with  $M_{\gamma_i}(s) = [1 - \Gamma_i s]^{-1}$  [19, Table 2.2], where from (19)

$$\Gamma_i \triangleq E\{\gamma_i\} = \frac{\frac{E_s}{N_0} \lambda_i |\mu_i|^2}{\frac{E_s}{N_0} \lambda_i (1 - |\mu_i|^2) + 1}. \quad (27)$$

Then, (26) yields the symbol-AEP expression for MPSK and exact MREC of order  $N$  as

$$P_{e,N} = \frac{1}{\pi} \int_0^{\frac{M-1}{M}\pi} \prod_{i=1}^N \left(1 + \Gamma_i \frac{g_{\text{PSK}}}{\sin^2 \phi}\right)^{-1} d\phi, \quad (28)$$

which depends on modulation constellation size, MREC order  $N$ , antenna correlation (i.e., also AS), and estimation method and parameters. Although (28) requires numerical integration, it can be computed easily, unlike the approximate MREC closed-form AEP expression (37). Note from (28) that the performance of exact MREC cannot degrade with an increasing number of eigenbranches because  $\Gamma_i > 0$ ,  $\forall i = 1 : N$ , unlike for approximate MREC [8].

2) *Relation to BF and MRC for Exact Combining:* For  $N = 1$ , exact MREC becomes exact BF, and then (28) is the exact-BF AEP expression. This can be shown to coincide with the approximate-BF AEP expression, i.e., Eqn. (37) written for  $N = 1$ . This is anticipated since approximate and exact BF coincide for our assumption of real-valued, positive, correlation coefficients.

For  $N = L$ , exact MREC is equivalent to exact MRC because the total SNR conditioned on the eigen-gain estimates given by (22) equals the corresponding MRC SNR, even for non-i.i.d. branches [10]. Thus, (28) with  $N = L$  describes exact-MRC performance.

3) *Relation to Ideal Eigen-/Combining:* For perfect channel knowledge we obtain  $\mu_i = 1$ ,  $\forall i = 1 : L$ . Then  $\Gamma_i$  from (27) becomes  $\check{\Gamma}_i \triangleq \frac{E_s}{N_0} \lambda_i$ , and (28) reduces to (7), i.e., the AEP expression for ideal MREC (and for ideal BF and MRC, as special cases) for correlated branches and MPSK modulation. Clearly,  $\Gamma_i$ ,  $\forall i = 1 : L$ , can be regarded as effective average SNRs. Thus, we unified the treatment of optimum eigen-/combining for perfectly- and imperfectly-known channel gains which can be non-i.i.d.

*E. Revisiting Approximate MRC for I.I.D. Gains and MPSK*

1) *New AEP Expression:* Consider the case of imperfectly-known channel and i.i.d. branches. MRC and full MREC obviously coincide. The factor which multiplies  $g_i$  in (23) to yield the exact-MRC weight is real-valued, positive, and the same  $\forall i = 1 : L$ , which reduces the exact-MRC weights to the approximate-MRC weights from (10). Then, Eqn. (24) represents a simple, novel, symbol error probability expression for MPSK and approximate MRC of i.i.d. branches, conditioned on the channel gains estimates, readily applicable for outage probability [19] calculations. The symbol-AEP expression follows from (28) as

$$P_{\text{approx MRC, i.i.d.}} = \frac{1}{\pi} \int_0^{\frac{M-1}{M}\pi} \left(1 + \Gamma_1 \frac{g_{\text{PSK}}}{\sin^2 \phi}\right)^{-L} d\phi, \quad (29)$$

since  $\Gamma_1 = \Gamma_2 = \dots = \Gamma_L$ . Note that approximate/exact MRC performance cannot degrade as more (i.i.d.) branches are added, because  $\Gamma_1 > 0$ .

Using [19, Appendix 5A.1], Eqn. (29) with  $M = 2$  can be shown to reduce to previous results for BPSK [7, Appendix C, Eqn. C-18], [8, Eqn. 38], [16, Eqn. 59], [21, Eqn. 23]. However, it is not known whether the analysis methods in [8], [16], [21] can be generalized for MPSK. Furthermore, for MPSK modulation, the new AEP expression (29) is much simpler than the only (incomplete, non-closed-form) alternative [7, Appendix C, Eqn. C-16] known to the authors. An involved closed-form equivalent of (29) can be obtained based on [19, Appendix 5A.3].

2) *Comparison with Previous Work:* We noticed intriguing similarities and differences between our approach in deriving (29), and previous results targeting BPSK and i.i.d. branches [21, Section III-A]:  $\Gamma_1$ , defined in (27), which enters our AEP expression (29), coincides with the “effective SNR due to Gaussian errors” defined in [21, Eqn. 22], which enters the AEP expression [21, Eqn. 23]. Further investigation reveals that a cumbersome model used previously to express the fading gain in terms of its estimate [21, Eqn. 8] (originally proposed in [17, Eqn. 16]) is actually equivalent to (17). However, [17], [21] do not focus on the conditioned SNR, as we did in Section III-D.1 — see Eqn. (22) — which leads to a complicated and apparently inaccurate AEP derivation in [18] (for the reason explained in [21, Section II]), as well as an additional averaging step in [21] (over  $V_1$  defined in [21, Eqn. 15], completed using [21, Eqn. 18]). The approach presented above in Section III-E.1 (and based on the derivations from Section III-D.1) is simpler and works for any MPSK constellation because  $\mathbf{e}$  from (17) is considered as noise, unlike in previous work [17], [21].

*F. Performance and Complexity Comparison*

Table II lists MRC and order- $N$  MREC per symbol complexities involved by KLT, interpolation, and combining. Interpolation vectors and eigen-decomposition computations have been neglected, since they need to be updated infrequently. Note that: 1) MREC complexity scales linearly with order; 2) unlike for MRC, MREC complexity is fairly invariant with the combining method, and invariant with the interpolation method, due to eigenbranch independence; 3) for MMSE

TABLE II

PER SYMBOL NUMERICAL COMPLEXITY (NO. OF COMPLEX MULTIPLICATIONS/ADDITIONS) FOR  $L$  BRANCHES.

Combining method	Interpolation method	MRC	order- $N$ MREC
approximate	SINC	$L(T+1)$	$N(L+T+1)$
	MMSE	$L(LT+1)$	$N(L+T+1)$
exact	SINC	$L(L+T+1)$	$N(L+T+2)$
	MMSE	$L(LT+L+1)$	$N(L+T+2)$

PSAM, MRC (performance-equivalent to full MREC) is much more complex than full MREC; 4) for SINC PSAM, MRC and full MREC have similar complexity for exact combining, while high-order MREC can be more complex than MRC for approximate combining.

For the same scenario as in Section II (BPSK, ULA,  $L = 5$ ,  $d_n = 1$ ,  $\theta_c = 0^\circ$ , Laplacian p.a.s.,  $f_m = 0.01$ ), symbol SNR  $E_s/N_0 = 5$  dB, and MMSE PSAM ( $M_s = 39$ ,  $T = 11$  [24]), the middle subplot of Fig. 1 shows the exact-MREC AEP versus AS. BF performs best for zero AS and poorly otherwise because it relies on branch coherence. MRC, which yields full diversity advantage, can significantly outperform BF for  $AS > 0$ . Nevertheless, for small AS, MRC yields BF-like performance for about 16 times higher complexity (see Table II). For larger AS, low-order MREC (with diversity advantage) can greatly outperform BF, and can achieve MRC/full-MREC (optimum) performance, for significantly lower complexity than that of MRC (see Table II): for  $AS < 6^\circ$ , order-2 MREC yields  $\approx 88\%$  savings, for  $6^\circ < AS < 12^\circ$ , order-3 MREC yields  $\approx 82\%$  savings, while for  $12^\circ < AS < 18^\circ$ , order-4 MREC yields  $\approx 76\%$  savings. For  $AS > 18^\circ$ , full MREC yields  $\approx 70\%$  savings over MRC. Recall that for the typical urban scenario described in Section II, the AS is small-to-moderate, i.e.,  $Pr(1^\circ < AS < 20^\circ) \approx 0.8$ , and slowly varying compared to channel fading [2], [3]. Hence, significant performance gains and complexity reductions over BF and MRC are possible by exploiting adaptive MREC with optimal order selection.

#### IV. OPTIMUM ORDER SELECTION FOR MREC

##### A. Previous Criteria

Drawing on previous results [12], a possible criterion for MREC adaptation is

$$\min_{N=1:L} E \left\{ E_s \cdot \|\mathbf{\Pi}_{L-N} \tilde{\mathbf{h}}\|^2 + \|\mathbf{\Pi}_N \tilde{\mathbf{n}}\|^2 \right\}, \quad (30)$$

where  $\|\cdot\|$  stands for Euclidian norm,  $\mathbf{\Pi}_N \triangleq \mathbf{E}_N \mathbf{E}_N^H$  is the orthogonal projection on the subspace spanned by the columns of  $\mathbf{E}_N$ , and  $\mathbf{\Pi}_{L-N} \triangleq \mathbf{I}_L - \mathbf{\Pi}_N$ . This criterion is equivalent to

$$\min_{N=1:L} \left[ E_s \cdot \sum_{i=N+1}^L \lambda_i + N_0 \cdot N \right] \quad (31)$$

and is better known as the *bias-variance tradeoff* criterion [12] (BVTC) because (31) balances the loss incurred by removing the weakest  $(L - N)$  intended-signal contributions (the first

term) against the residual-noise contribution (the second term). Although applicable for both approximate-MREC [12] and exact-MREC [10], BVTC does not account for the actual combining approach, Doppler rate, channel estimation method and its parameters ( $M_s$ ,  $T$ ). Furthermore, the BVTC requires knowledge of the smallest eigenvalues, which may be inaccurately estimated.

To ensure that the selected order depends on the estimation method and parameters, Dietrich *et al.* [14] applied the following MMSE criterion (MMSEC)

$$\min_{N=1:L} E \left\{ \|\tilde{\mathbf{h}} - \mathbf{E}_N \mathbf{g}\|^2 \right\} \quad (32)$$

for order selection in approximate MREC. However, it was found that the MMSEC output does not minimize the AEP for maximum-likelihood eigengain estimation [14, Section VI] or for SINC PSAM [10]. Furthermore, the MMSEC cannot reduce dimension for MMSE PSAM, regardless of antenna correlation, symbol SNR or fading rate [10].

A common, important, BVTC and MMSEC drawback is disregard of ensuing MREC complexity and symbol-detection performance. These criteria can thus 1) waste processing resources on inaccurately estimating insignificant eigengains and on high-dimensional combining, or 2) ignore eigen-directions with needed performance-enhancing potential.

##### B. Proposed Performance-Complexity Tradeoff Criterion (PCTC)

For Rayleigh fading and MPSK, the AEP of exact MREC given by (28) is a non-increasing function of the MREC order,  $N$ . Furthermore, since  $\sin^2 \phi \leq 1$ , Eqn. (28) implies

$$P_{e,N} \leq \frac{P_{e,N-1}}{1 + \Gamma_N \cdot \sin^2 \frac{\pi}{M}}, \quad (33)$$

i.e., order- $N$  MREC will guarantee an AEP decrease by the factor  $[1 + \Gamma_N \cdot \sin^2 \frac{\pi}{M}]$  over order- $(N - 1)$  MREC. This decrease is larger for smaller signal constellation sizes as well as for larger  $\Gamma_N$ . However, this performance improvement may not be worth the extra computational complexity of estimating the additional eigengain. Therefore, we propose the following performance-complexity tradeoff criterion (PCTC): use the  $N$ th eigenbranch only if it guarantees

$$P_{e,N} \leq v \cdot P_{e,N-1}, \quad (34)$$

where  $v \in (0, 1)$  is a design parameter chosen based on eigengain estimation complexity and receiver processing load. A *sufficient* condition for (34) to hold is that

$$\Gamma_N \geq \Gamma_c \triangleq \frac{(v^{-1} - 1)}{\sin^2 \frac{\pi}{M}}, \quad (35)$$

where  $\Gamma_c$  is the *cutoff* average conditioned SNR. (The derivation of the *necessary* condition for (34) is not tractable). The PCTC selects as MREC order the largest value of  $N$  for which (35) holds. (Note that, unlike the BVTC-based approach, the PCTC may not require knowledge of weak eigenvalues, whose estimates may be inaccurate.) When the channel conditions are so poor that  $\Gamma_2 \not\geq \Gamma_c$ , the receiver will deploy BF. Otherwise, higher-order MREC is selected. For very good channel conditions, the MREC order  $N$  output by

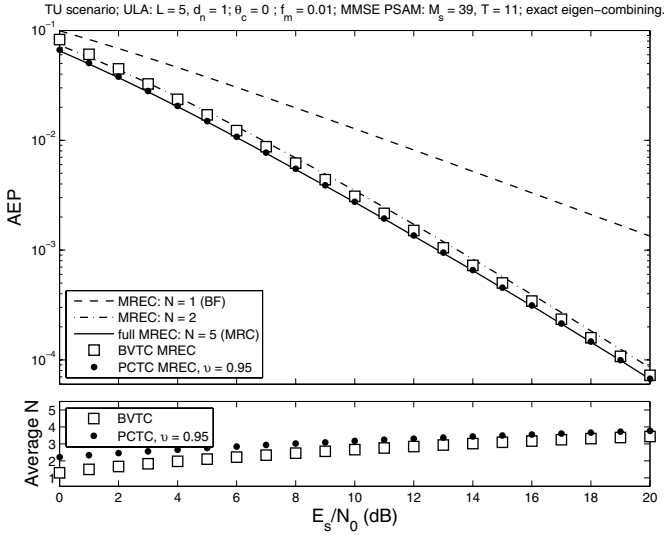


Fig. 2. Top: AEP for BPSK, MMSE PSAM, and exact MREC vs. the SNR per symbol, averaged over 10,000 independent samples of log-normal AS for a TU scenario; the results for MREC of order  $N = 3, 4$  (not shown) approach those for full MREC. Bottom: MREC order selected with discussed criteria. Higher symbol-SNR leads to better performance but also higher complexity.

our criterion may approach or equal  $L$ . The above PCTC needs to be supplemented with a condition for switching from order- $N$  MREC to MRC only if MREC complexity can become higher than MRC complexity, which is not the case considered hereafter.

In Fig. 1, the bottom subplot shows the MREC order selected with the PCTC for  $\nu = 0.95$ , and with the BVTC. The corresponding AEP values for adapted MREC appear in the middle subplot. For this choice of  $\nu$ , the proposed PCTC outperforms the BVTC, at the price of higher complexity. The situation may reverse when complexity is more important, i.e., for smaller  $\nu$ . The effectiveness of the PCTC-based MREC is evident at  $AS = 10^\circ$ , where MREC yields almost the same (lowest) AEP for  $3 \leq N \leq L = 5$ , but  $N = 3$  is selected, to minimize complexity. The BVTC selects  $N = 2$ , even though the performance may be unacceptable and sufficient processing resources may still be available. The SNR thresholds for a PCTC-based MREC receiver can be adapted to the base station load, so that they increase before the signal processing resources are exhausted, thus yielding higher user capacity and graceful performance degradation.

## V. NUMERICAL RESULTS FOR RANDOM AZIMUTH SPREAD

For the same scenario as before, we generated 10,000 independent log-normal AS samples using (2). The AS average and standard deviation were  $9.76^\circ$  and  $13.43^\circ$ , respectively. The correlation matrix  $\mathbf{R}_{\tilde{\mathbf{h}}}$  and its eigenvalues were computed at every sample, and the exact-MREC AEP was computed using (28) for MMSE PSAM. Fig. 2 shows that PCTC-based MREC performs significantly better than BF (e.g., almost 5 dB at  $AEP = 10^{-2}$ , and more than 7 dB at  $AEP \approx 10^{-3}$ ), and as well as full MREC and MRC. Note that higher MREC order is selected for increasing SNR. Fig. 2 and Table II indicate that, for symbol-SNR in the range  $[0 \text{ dB}, 10 \text{ dB}]$ , PCTC-based

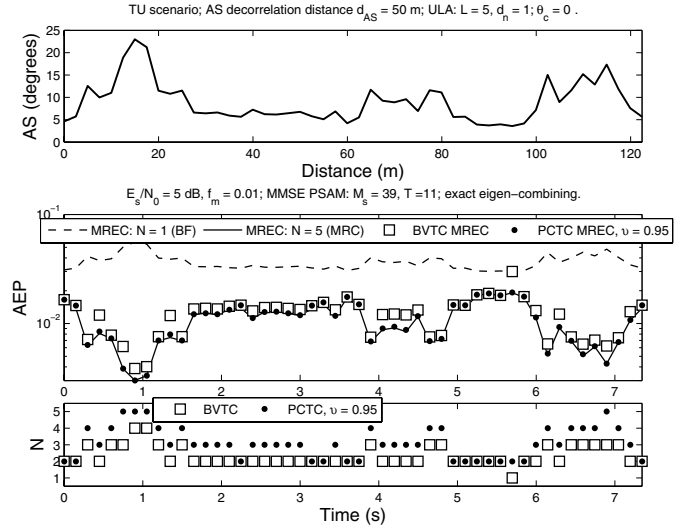


Fig. 3. Top: AS vs. distance traveled by mobile station, for a TU scenario; Middle: AEP for BPSK, MMSE PSAM, and exact BF, MRC, and adaptive MREC, vs. time; Bottom: adaptively-selected MREC order vs. time. The PCTC adaptively selects the MREC order which ensures the best performance for a designer-approved complexity level.

adaptive exact MREC achieves optimum performance (i.e., the exact-MRC performance) for about 80% – 90% lower complexity than that of exact MRC.

The top subplot in Fig. 3 displays the AS computed using (2), (3). The mobile station travels a 125 m distance in 7.5 s and transmits 75,000 symbols. To emulate actual updating,  $\mathbf{R}_{\tilde{\mathbf{h}}}$  and its eigenstructure are recalculated once every  $d_{AS}/20 = 2.5 \text{ m}$  (or 1500 symbols). Over this distance there is small AS variation, and sufficient independent signal samples would be available for actual eigenstructure estimation. Fig. 3 shows in the middle subplot the BF, MRC, and adaptive MREC AEPs evaluated using (28) after each eigenstructure update, and in the lower subplot the MREC orders selected adaptively with the applicable criteria described in Section IV. Adaptive PCTC-based MREC can lead to significant performance gain and complexity reduction over BF and MRC, respectively. Simulations of this scenario when  $\mathbf{R}_{\tilde{\mathbf{h}}}$  and its eigenstructure are recursively updated confirm these results. Numerical results from [8], [10] indicate that the PCTC from (35) is effective also for approximate-MREC adaptation.

## VI. CONCLUSIONS

The performance and complexity of optimal (exact) and suboptimal (approximate) eigen-/combining are analyzed for PSK transmitted signal, and imperfectly-known Rayleigh fading channel gains which can be correlated and non-identically distributed. The claim that exact/approximate maximal-ratio eigen-combining (MREC) is a superset of maximum average signal-to-noise ratio beamforming (BF) and maximal-ratio combining (MRC) is proved for pilot-based estimated channels. A new, simple, average error probability (AEP) expression for approximate MRC of i.i.d. branches and MPSK is derived using exact-MRC analysis.

The flexibility of MREC can be advantageously harnessed for controlled performance adjustments as users enter and

leave the system. A new performance–complexity tradeoff criterion for MREC-adaptation to channels with variable spatial scattering is proposed and evaluated for a typical urban mobile scenario which is characterized by Laplacian power azimuth spectrum with log-normal, small-to-moderate, azimuth spread. We found that a compact, 5-element, adaptive exact-MREC antenna array can outperform a BF antenna array by about 5–7 dB, at  $AEP \in [10^{-2}, 10^{-3}]$ . Furthermore, for symbol-SNR in the range [0 dB, 10 dB], adaptive exact-MREC can achieve optimum performance (i.e., the exact-MRC performance) for about 80% – 90% lower complexity than that of exact MRC. Smarter, MREC-based, scattering-aware, antenna arrays can thus significantly benefit mobile wireless communication systems.

#### APPENDIX

##### CLOSED-FORM AEP EXPRESSION FOR BPSK AND APPROXIMATE MREC

Let us assume BPSK transmission of symbol  $b = 1$ . Then, it can be shown [8, Section III.A], [10] that for the test variable  $q$  from (11) we can write

$$M_q(-s) \triangleq E\{e^{-sq}\} = \prod_{k=1}^{N_d} \frac{1}{[-a_k^2(s - s_{k,1})(s + s_{k,2})]^{r_k}},$$

with  $\sum_{k=1}^{N_d} r_k = N$ ,

$$a_k^2 = \frac{1}{4} N_0 \sigma_{g_k}^2 [1 + (1 - \mu_k^2) \check{\Gamma}_k] > 0,$$

with  $\check{\Gamma}_k$  defined in Section III-D.3, and

$$s_{k,1}, s_{k,2} = \frac{2\check{\xi}_k}{\sqrt{E_s \sigma_{h_k}^2 \sigma_{g_k}^2}} \cdot \frac{1}{1 \mp \mu_k \check{\xi}_k} > 0,$$

with  $\check{\xi}_k = \sqrt{\frac{\check{\Gamma}_k}{\Gamma_{k+1}}}$ . Above,  $(s_{k,1}, -s_{k,2})$  represent the  $k$ th — out of  $N_d$  — distinct pole pairs of  $M_q(-s)$ , and  $r_k$  is the corresponding algebraic multiplicity.

Then, the p.d.f. of  $q$  is given by

$$p_q(\alpha) \triangleq \int_{-\infty}^{\infty} e^{s\alpha} M_q(-s) ds. \quad (36)$$

and the average error probability is given by  $P_e = Pr(q < 0)$ , i.e., [8, Section III.A.1, pp. 18-19], [10]

$$P_e = \frac{1}{B} \sum_{k=1}^{N_d} \sum_{l=1}^{r_k} c_{k,l} \cdot \left[ -\frac{\sqrt{E_s \sigma_{h_k}^2 \sigma_{g_k}^2}}{\check{\xi}_k} \cdot \frac{1 - \mu_k \check{\xi}_k}{2} \right]^l \quad (37)$$

with

$$B = \prod_{k=1}^{N_d} (-a_k^2)^{r_k}, \quad (38)$$

$$c_{p,l} = (-1)^{\rho_p - l} \cdot \sum_{\Psi} \prod_{\substack{j=1 \\ j \neq p}}^{2N_d} \delta_j \cdot \frac{1}{(\sigma_j - \sigma_p)^{\rho_j + i_j}}, \quad (39)$$

where  $\Psi$  stands for the set of integers  $i_j$ , satisfying  $0 \leq i_j \leq \rho_p - l$ ,  $\forall j \neq p$ , and  $\sum_{\substack{j=1 \\ j \neq p}}^{2N_d} i_j = \rho_p - l$ ,  $\delta_j = \binom{\rho_j - 1 + i_j}{i_j}$ , while  $\sigma_p = -s_{p,1}$ ,  $\rho_p = r_p$ , for  $p = 1 : N_d$ , and  $\sigma_p = s_{p-N_d,2}$ ,  $\rho_p = r_{p-N_d}$ , for  $p = N_d + 1 : 2N_d$ .

#### REFERENCES

- [1] J. Salz and J. H. Winters, "Effect of fading correlation on adaptive arrays in digital mobile radio," *IEEE Trans. Vehic. Technol.*, vol. 43, no. 4, pp. 1049–1057, Nov. 1994.
- [2] K. I. Pedersen, P. E. Mogensen, and B. H. Fleury, "A stochastic model of the temporal and azimuthal dispersion seen at the base station in outdoor propagation environments," *IEEE Trans. Veh. Technol.*, vol. 49, no. 2, pp. 437–447, Mar. 2000.
- [3] A. Algans, K. I. Pedersen, and P. E. Mogensen, "Experimental analysis of the joint statistical properties of azimuth spread, delay spread and shadow fading," *IEEE J. Select. Areas Commun.*, vol. 20, no. 23, pp. 523–531, Apr. 2002.
- [4] L. Schumacher, K. I. Pedersen, and P. E. Mogensen, "From antenna spacings to theoretical capacities - guidelines for simulating MIMO systems," in *Proc. IEEE Int. Symp. on Pers., Indoor and Mobile Radio Commun. (PIMRC'02)*, vol. 2, 2002, pp. 587–592.
- [5] R. A. Monzingo and T. W. Miller, *Introduction to Adaptive Arrays*. New York, NY: John Wiley, 1980.
- [6] D. G. Brennan, "Linear diversity combining techniques," *Proc. IEEE*, vol. 91, no. 2, pp. 331–356, Feb. 2003.
- [7] J. H. Proakis, *Digital Communications, 4th Edition*. Boston, MA: McGraw-Hill, 2001.
- [8] C. Siriteanu and S. D. Blostein, "Maximal-ratio eigen-combining: a performance analysis," *Canadian J. Elec. and Comp. Eng.*, vol. 29, no. 1/2, pp. 15–22, Jan./Apr. 2004.
- [9] C. Siriteanu and S. D. Blostein, "Smart antenna arrays for correlated and imperfectly-estimated Rayleigh fading channels," in *Proc. IEEE Int'l. Conf. on Commun. (ICC'04)*, vol. 5, 2004, pp. 2757–2761.
- [10] C. Siriteanu, "Maximal-ratio eigen-combining for smarter antenna array wireless communication receivers," Ph.D. dissertation, Queen's University, Kingston, Ontario, Canada, Aug. 2006.
- [11] C. Brunner, W. Utschick, and J. A. Nossek, "Exploiting the short-term and long-term channel properties in space and time: eigenbeamforming concepts for the BS in WCDMA," *European Trans. Telecommun. Special Issue on Smart Antennas*, vol. 12, no. 5, pp. 365–378, 2001.
- [12] J. Jelitto and G. Fettweis, "Reduced dimension space-time processing for multi-antenna wireless systems," *IEEE Wireless Commun. Mag.*, vol. 9, no. 6, pp. 18–25, Dec. 2002.
- [13] M. Kim *et al.*, "Adaptive beamforming technique based on eigen-space method for a smart antenna in IS2000 1X environment," in *Proc. IEEE Ant. and Prop. Soc. Int'l. Symp.*, vol. 1, 2002, pp. 118–121.
- [14] F. A. Dietrich and W. Utschick, "On effective spatio-temporal rank of wireless communication channels," in *Proc. IEEE Int'l. Symp. Pers. Indoor and Mobile Radio Commun., (PIMRC'02)*, vol. 5, 2002, pp. 1982–1986.
- [15] F. A. Dietrich and W. Utschick, "Maximum ratio combining of correlated Rayleigh fading channels with imperfect channel knowledge," *IEEE Commun. Lett.*, vol. 7, no. 9, pp. 419–421, Sept. 2003.
- [16] P. Bello and B. D. Nelin, "Predetection diversity combining with selectively fading channels," *IEEE Trans. Commun.*, vol. 10, no. 1, pp. 32–42, Mar. 1962.
- [17] M. J. Gans, "The effect of Gaussian error in maximal ratio combiners," *IEEE Trans. Commun.*, vol. COM-19, no. 4, pp. 492–500, Aug. 1971.
- [18] B. R. Tomiuk, N. C. Beaulieu, and A. A. Abu-Dayya, "General forms for maximal ratio diversity with weighting errors," *IEEE Trans. Commun.*, vol. 47, no. 4, pp. 488–492, Apr. 1999.
- [19] M. K. Simon and M.-S. Alouini, *Digital communication over fading channels: a unified approach to performance analysis*. New York, NY: John Wiley and Sons, 2000.
- [20] P. Shamain and L. B. Milstein, "Detection with spatial diversity using noisy channel estimates in correlated fading channel," in *Proc. IEEE Mil. Commun. Conf. (MILCOM'02)*, vol. 1, 2002, pp. 691–696.
- [21] R. Annavajjala and L. B. Milstein, "On the performance of diversity combining schemes on Rayleigh fading channels with noisy channel estimates," in *Proc. IEEE Mil. Commun. Conf. (MILCOM'03)*, vol. 1, 2003, pp. 320–325.
- [22] R. Annavajjala, "A simple approach to error probability with binary signaling over generalized fading channels with maximal ratio combining and noisy channel estimates," *IEEE Trans. Wireless Commun.*, vol. 4, no. 2, pp. 380–383, Mar. 2005.
- [23] P. Polydorou and P. Ho, "Error performance of MPSK with diversity combining in non-uniform Rayleigh fading and non-ideal channel estimation," in *Proc. IEEE Vehic. Technol. Conf., (VTC Spring'00)*, vol. 1, 2000, pp. 627–631.
- [24] J. K. Cavers, "An analysis of pilot symbol assisted modulation for Rayleigh fading channels," *IEEE Trans. Vehic. Technol.*, vol. 40, no. 4, pp. 686–693, Nov. 1991.

- [25] T. S. Rappaport, *Wireless Communications. Principles and Practice*. Upper Saddle River, NJ: Prentice-Hall, 1996.
- [26] X. Dong and N. C. Beaulieu, "Optimal maximal ratio combining with correlated diversity branches," *IEEE Commun. Lett.*, vol. 6, no. 1, pp. 22–24, Jan. 2002.
- [27] S. Loyka *et al.*, "Comments on 'New method of performance analysis for diversity reception with correlated Rayleigh-fading signals'," *IEEE Trans. Vehic. Technol.*, vol. 52, no. 6, pp. 725–726, May 2003.
- [28] S. M. Kay, *Fundamentals of Statistical Signal Processing. Estimation Theory*. Englewood Cliffs, NJ: Prentice-Hall, 1993.



**Steven D. Blostein** received his B.S. degree in Electrical Engineering from Cornell University, Ithaca, NY, in 1983, and the M.S. and Ph.D. degrees in Electrical and Computer Engineering from the University of Illinois, Urbana-Champaign, in 1985 and 1988, respectively. He has been on the Faculty at Queen's University since 1988 and currently holds the position of Professor and Head of the Department of Electrical and Computer Engineering. From 1999-2003, he was the leader of the Multirate Wireless Data Access Major Project sponsored by the Canadian Institute for Telecommunications Research. He has also been a consultant to industry and government in the areas of image compression and target tracking, and was a Visiting Associate Professor in the department of Electrical Engineering at McGill University in 1995. His current interests lie in the application of signal processing to wireless communications systems, including smart antennas, MIMO systems, and space-time frequency processing for MIMO-OFDM systems. He served as Chair of IEEE Kingston Section in 1993-94, Chair of the Biennial Symposium on Communications in 2000 and 2006, and as Associate Editor for IEEE Transactions on Image Processing from 1996-2000.



**Constantin (Costi) Siriteanu** was born in Sibiu, Romania, in 1972. He received his B.S. and M.S. degrees in Electrical Engineering, from "Gheorghe Asachi" Technical University, Iasi, Romania, in 1995 and 1996, respectively, and the Ph.D. degree from Queen's University, Kingston, Canada, in 2006.

Between 1995 and 1997 he was part-time engineer with the Research Institute for Automation, Iasi, Romania, working on data transmission over power lines. Between 1996 and 1998 he was Research Assistant with the Department of Automatic Control and Computer Science, "Gheorghe Asachi" Technical University, Iasi, Romania, working on digital control systems.

Between 1998 and 2006, he was Research Assistant and Course Instructor with the Department of Electrical and Computer Engineering, Queen's University, Kingston, Canada. His Ph.D. research focused on adaptive signal processing for smart antenna array receivers, and especially on performance-complexity tradeoffs based on channel statistics.

Since September 2006, he has been post-doctoral fellow with the HY-SDR (Hanyang Software-Defined Radio) Research Centre, at Hanyang Institute of Technology, Hanyang University, Seoul, South Korea, working on smart antenna signal processing for OFDM systems such as WiMAX and WiBro.